Scripta Materialia 156 (2018) 134–137

Contents lists available at ScienceDirect

Scripta Materialia

journal homepage: www.elsevier.com/locate/scriptamat

Regular article

A promising high-efficiency photovoltaic alternative non-silicon material: A first-principle investigation

Murugesan Rasukkannu [a,*], Dhayalan Velauthapillai [a], Vajeeston Ponniah [b]

[a] Western Norway University of Applied Sciences, Department of Computing, Mathematics and Physics, Inndalsveien 28, Box 5063, Bergen, Norway
[b] Center for Materials Science and Nanotechnology, Department of Chemistry, University of Oslo, Box 1033, Blindern, N-0315 Oslo, Norway

ARTICLE INFO

Article history:
Received 8 July 2018
Received in revised form 19 July 2018
Accepted 20 July 2018
Available online xxxx

Keywords:
HSE06
PV materials
Hybrid density function
$TlBiS_2$
Non-silicon solar cell material

ABSTRACT

We demonstrate by means of first-principle calculations that the band structure of $TlBiS_2$ characterizes this material as a promising candidate for photovoltaic applications. Two calculation hybrid functional models are used, one including the spin-orbit coupling and one neglecting it. These calculations show that $TlBiS_2$ has a direct band gap of 1.10 eV in the absence of spin-orbit coupling and 0.67 eV for spin-orbit coupling. The absorption peaks appear in the visible region with a consequently high absorption intensity for both without and with spin-orbit coupling. We show how computational modeling of $TlBiS_2$ can substantially enrich the understanding of photovoltaic properties.

Silicon devices are currently the dominating technology for photovoltaic applications. More than 80% of the solar cell modules installed worldwide are based on either mono or multi-crystalline silicon. However, silicon exhibits an indirect band gap, resulting in a low absorption coefficient [1]. The research community has thus been making efforts in studying alternative materials for photovoltaic applications. Ternary, binary, multinary materials and compounds such as copper zinc tin sulfide, characterized by direct band gap and high absorption coefficient, are of utmost interest for photovoltaic application. The desirable features of alternative materials are high photon conversion efficiencies and low production cost. The chalcogenide-structured narrow band semiconducting compounds with general valence types III-V-VI_2, V_2-VI_3 (where III = Al, Ga, In, Tl; V = P, As, Sb, Bi; VI = Se, Te, S) have been investigated due to their application as topological insulator [2–6] and have not been widely investigated in solar cell. Topological insulators are innovative materials represent an ideal platform for nanoelectronics, optoelectronics and photonics [5–9].

The relative cost and scarcity of Ga and In have motivated a drive for alternative materials for photovoltaic applications. Thallium-bearing ternary semiconductors have been investigated in optoelectronics [10], but not extensively studied in photovoltaics due to the toxicity of thallium. However, $TlBiS_2$ have strong absorption coefficient with an optimum band gap, resulting in high efficiency for the photovoltaic process. $TlBiS_2$ crystallizes with a chalcogenide-structure, and it exhibits a narrow band gap with valence band and conduction bands located at Γ and F-point of the Brillouin zone [2]. The electronic properties of $TlBiS_2$ are already well studied using *ab initio* calculations under the generalized gradient approximation (GGA) [2, 11]. However, accurate Heyd-Scuseria-Ernzerhof (HSE06) and Bethe-Salpeter equation (BSE) calculation have not yet been used to explore its photovoltaic properties. This is addressed here by calculating the electronic band structure and optical properties of III-V-VI_2 compound (III = Tl, V = Bi, VI = S), as well as the effective masses.

Total energies have been calculated by the projected augmented plane-wave (PAW) implementation of the Vienna *ab initio* simulation package (VASP) [12, 13]. Structural optimization calculations are performed using the Perdew-Burke-Ernzerhof (PBE) version of the generalized gradient approximation (GGA) of the exchange-correlation functional [14]. The convergence threshold for self-consistent calculations is set to 10^{-6} eV, the atomic positions and lattice were fully optimized by minimizing the stress tensor and the Hellman-Feynman forces using the conjugate-gradient algorithm with a force convergence threshold of 10^{-3} eV $Å^{-1}$. We used the hybrid non-local exchange-correlation functional of Heyd-Scuseria-Ernzerhof (HSE06) to calculate the electronic structure [15]. The spin-orbit coupling was included in the calculations with non-collinear spins. In the HSE06 method, the screened parameter is set to 0.2 $Å^{-1,}$ and 30% of the screened Hartree-Fock (HF) exchange is mixed with the PBE exchange functional [16]. The cut-off energy for the plane-wave basis set is 600 eV, and we use a 10 × 10 × 10 Γ-centered Monkhorst-pack **k**-point mesh to sample the Brillouin zone [17]. This setup is maintained for both PBE and HSE06 calculations. Solving of the Casida's equation is an alternative,

* Corresponding author.
E-mail addresses: rmu@hvl.no (M. Rasukkannu), vdh@hvl.no (D. Velauthapillai), ponniahv@kjemi.uio.no (V. Ponniah).

https://doi.org/10.1016/j.scriptamat.2018.07.027
1359-6462/

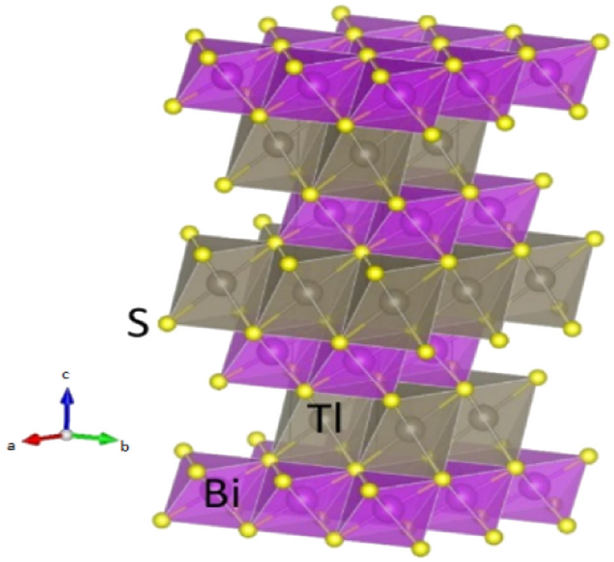

Fig. 1. Crystal structures for $TlBiS_2$. The labels for the different kinds of atoms are shown in the illustration.

well-established approach for calculating the dielectric function [18]. For both GW and the Bethe-Salpeter equation (BSE), we have summed the contributions over a number of $8 \times 8 \times 8$ **k**-points grids, shifted with respect to each other to reproduce $16 \times 16 \times 16$ Γ-centered grid. For all these calculations, a plane-wave cutoff of 410 eV has been used.

The structure of $TlBiS_2$ is closely related to ABQ_2-type compounds (A = monovalent atom, B = trivalent atom and Q = chalcogen) and can be derived from a simple NaCl-type lattice by a rhombohedral distortion along the [111] direction, corresponding to the c axis of the primitive hexagonal arrangement. The sum of the ionic radii for a coordination number (CN) of 6 is 2.87 Å for Bi^{3+}/S^{2-} and 3.34 Å for Tl^{+}/S^{2-} [$r(Bi^{3+}) = 1.03$ Å, $r(Tl^{+}) = 1.50$ Å and $r(S^{2-}) = 1.84$ Å] [19]. The experimentally determined and the theoretically derived values of the bond length are in good agreement for Bi—S, but for the Tl—S distance is underestimated by about 5.3%. The considered system has a rhombohedral crystal structure with four atoms in the primitive unit cell. The space group is D5 3d (R-3m, SG no. 166). The conventional hexagonal unit cell has 12 atoms corresponding to three formula units in which the layers are stacked in the order Tl-S-Bi-S along the z-axis. Each Tl (Bi) layer is sandwiched between the two S layers so that the bonding between all the layers is strong, and the material is essentially three-dimensional. Our calculated lattice parameters and the atomic positions are in good agreement with the experimental findings. The crystal structure of $TlBiS_2$ is presented in Fig. 1.

The band gap of the photoactive semiconductors determines the upper bound on the short-circuit current and open-circuit voltage. A large-band gap cell has a larger open-circuit voltage, and lower short-circuit current than a small-band gap cell. Thus, it absorbs fewer solar photons than a small-band gap cell. However, the detailed-balance limiting efficiency of an ideal solar cell of optimal band gap $E_g = 1.4$ eV is 32%. In real cells, thermalization loss occurs because the solar resource used has a broad energy spectrum, and it poorly matches the band gap, resulting in lower efficiencies below the detailed-balance limit [20]. Since the efficiency of solar cell is highly dependent on the band gap of material, the use of electronic band structure presents itself as a promising opportunity for engineering the material for photovoltaic applications. Fig. 2a shows the HSE06 band structure of $TlBiS_2$ without spin-orbit coupling. The valence band maximum (VBM) and the conduction band minimum (CBM) are located at the Γ **k**-point, characterising $TlBiS_2$ as a direct band gap semiconductor. The calculated HSE06 band gap between VBM and CBM is 1.1 eV. It is approximately equal to the silicon band gap, but of a different type. Bahadur Singh et al., used GGA calculation and showed that $TlBiS_2$ is a direct band gap semiconductor at Γ **k**-point, with a band gap of 0.64 eV [11]. The comparison between the present results using HSE06 with these previous GGA results [11] suggests that band gap of $TlBiS_2$ is larger by approximately 0.46 eV. It is well known that calculations using GGA underestimate the band gap value, while the HSE06 screened hybrid functional is very successful in accurately calculating it. At the F **k**-point, the band gap between VBM and CBM is 1.42 eV. The electronic structure studies of $TlBiS_2$ are identified, the direct band gap and 1.1 eV band gap for the solar cell application.

The spin-orbit coupling (SOC) is strongest for heavy elements, where the electrons acquire large velocities in the proximity of the nucleus. It may be suspected that a strong SOC effect, characteristic of heavy Bi, might be involved in affecting the properties of the material under examination. Therefore, we compare our previously obtained HSE06 band structure with results including the SOC. We may expect that the effect of SOC is of major importance for the distributions of the near-Fermi electronic states. Fig. 2b shows the HSE06 band structure of $TlBiS_2$ with spin-orbit coupling. In $TlBiS_2$, both the valence band maximum (VBM) and conduction band minimum (CBM) are located at the Γ **k**-point. Thus, $TlBiS_2$ is once again found to be a direct band gap semiconductor. The calculated HSE06 band gap between VBM and CBM is 0.67 eV. When we include SOC, the band gap shrinks significantly, and a similarly large energy shift is obtained for all bands throughout the Brillouin zone. Similar phenomena were observed by Bahadur Singh et al., when they band structure calculation including SOC, where the band gap was shown to shrink from 0.64 eV to 0.26 eV at Γ [11]. At the F **k**-point, the band gap between VBM and CBM is 1.16 eV. From Fig. 2a and Fig. 2b, we observe that the presence of SOC introduces large energy shift for all band, and the band gap values shrink

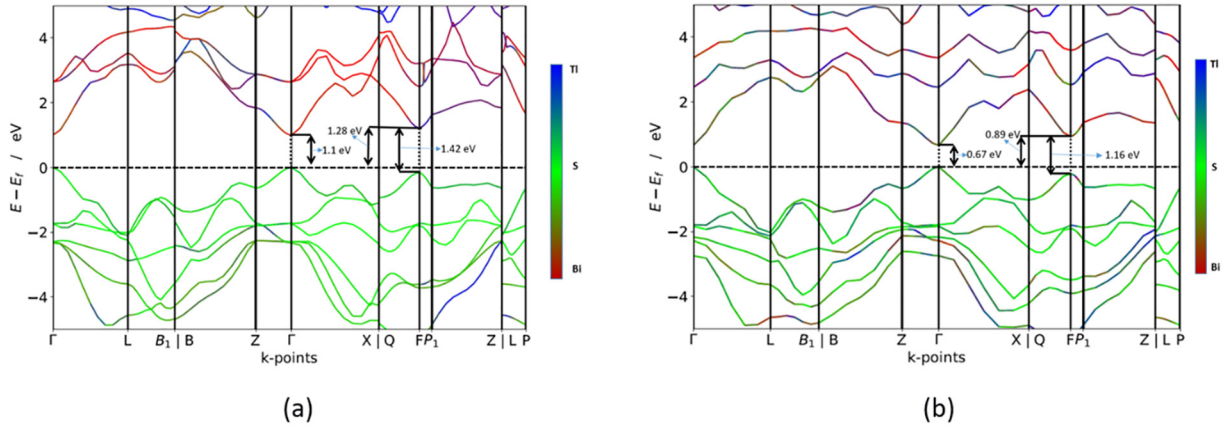

Fig. 2. Calculated HSE06 electronic band structure of $TlBiS_2$ (a) without spin-orbit coupling (b) with spin-orbit coupling. The Fermi level is set to zero.